Electric Field Effects on One-Bond Indirect Spin−Spin Coupling Constants and Possible Biomolecular Perspectives

Aleksandr B. Sahakyan,* Aleksan G. Shahkhatuni, Astghik A. Shahkhatuni, and Henry A. Panosyan

Molecule Structure Research Center of National Academy of Sciences, Yerevan 0014, Armenia

Received: January 23, 2008; In Final Form: February 25, 2008

Electric field (EF) induced changes of one-bond indirect spin−spin coupling constants are investigated on a wide range of molecules including peptide models. EFs were both externally applied and internally calculated without external EF application by the hybrid density functional theory method. Reliable agreement with experimental data has been obtained for calculated one-bond *J*-couplings. The role of the EF sign and direction, internal and induced components, hydrogen bonding, internuclear distance and hyperconjugative interactions on the one-bond *J*-coupling vs EF interconnection is analyzed. A linear dependence of ^1J on EF projection along the bond is obtained, if the bound atoms possess different enough electron densities and an EF determined by the electronic polarization exists along the bond. Accentuating the $^1J_{NH}$ couplings as possible EF sensitive parameters, a systematic study is done in two sets of molecules with a large variation of the native internal EF value. The most EF affected component of the $^1J_{NH}$ coupling constant is the spin-dipole term of Ramsey's formulation; however, in the total *J*-coupling formation, the EF influence on the Fermi contact term is the most significant. The induced EF projection along the bond is 6.7 times weaker in magnitude than the simulated external uniform field. The absolute EF dependence of the one-bond *J*-coupling involves only the internal field, which is the sum of the induced field (if the external field exists) and the internuclear field determined by the native polarization. That linear and universal dependence joins the corresponding couplings in a diverse set of molecules under various electrostatic conditions. Many types of the one-bond *J*-couplings can be potentially measured in biomolecules, and the study of their relation with the electrostatic properties at the corresponding sites opens a new avenue to the full exploitation of the NMR measurable parameters with novel and exciting applications.

1. Introduction

During the last decades NMR spectroscopy opened its boundless opportunities and became one of the main tools of molecular structure determination. Its measurable parameters, originating from the very inner core of the molecules, contain a wealth of information on both the molecular and the electronic structure and properties,[1−4] being sensitive to environmental influences as well.

Electric fields (EFs) as a common way of the long-range molecular "communication" are an undividable constituent of the molecular interactions and the solvent effects on the solute molecule. Electric dipoles, localized charges, electromagnetic radiation, polarized molecules and the investigated molecule itself are the sources of the EFs, which can alter both the chemical shifts and the indirect spin−spin couplings of the molecule.

The majority of research devoted to the EF effects on the NMR parameters refers to the chemical shifts[5−9] and the corresponding dependence for a diatomic molecule can be represented by the expression proposed by Buckingham:

$$\delta = \delta_0 - aF_{II} - bF_{II}^2 \qquad (1)$$

where δ and δ_0 are chemical shifts with and without EF, F_{II} is the EF parallel to the bond, a and b are the coefficients describing the bond dipole and the polarizability. The main influence on the chemical shifts has the first EF-coupled term in the equation, thus, in general, a linear dependence can be stated.[6] Unlike the chemical shifts, the problem of the EF effect on the indirect spin−spin coupling constants is not well studied; however, a linear *J*-coupling vs EF dependence was indicated for the $^1J_{CH}$ and $^3J_{HH}$ couplings in several fluorocarbohydrides,[10] for $^1J_{CH}$ coupling of the formyl group in various substituted salicylaldehydes[11] and for methylic $^2J_{HH}$ couplings in several substituted methanes.[12] In the latter work, the transferability of the eq 1 to the indirect spin−spin coupling constants was proposed. The potential of the formyl $^1J_{CH}$ coupling to serve as an adequate probe of intramolecular EFs was outlined.[11]

The existence of a linear dependence between the NMR measurable parameters and an EF is of great importance, if we consider the perspective of the use of NMR spectroscopy to measure EFs at the corresponding sites of the molecule.

EFs play a pivotal role in biomolecular processes. They influence nearly all the aspects of protein function: from driving the folding process to the key role in the molecular (macromolecule−ligand and protein−protein) recognition. EFs with a proper magnitude and direction at the active site of the enzymes determine their activity, reducing the activation barrier of the substrate modification and stabilizing the transition state.[13] Effects of the environment and mutations on protein electric properties are also of primary interest and their study can spread

* Corresponding author. E-mail: aleksahak@msrc.am. Tel: 37410-287423. Fax: 37410-282267.

10.1021/jp800670y CCC: $40.75
Published on Web 03/26/2008

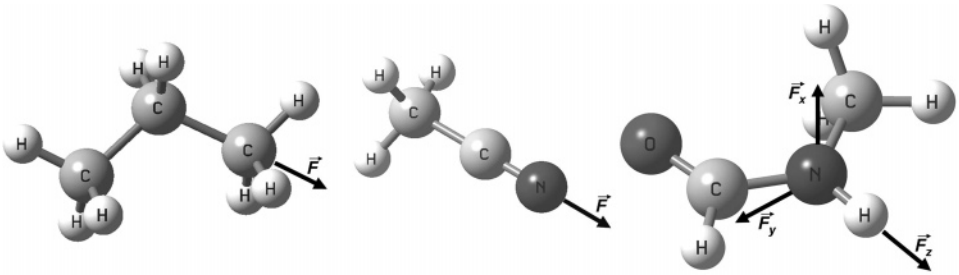

Figure 1. Propane, acetonitrile and *N*-methylformamide molecule with indicated applied electric field directions.

light on understanding many pathological processes, such us hereditary disorders and crucial protein aggregation.

Despite the importance of the issue, there are very few experimental methods for EF detection in biomolecules. The interconnection between the EFs in biomolecules and the chemical shifts was demonstrated by Oldfield et al.,[14] where a strong correlation was found between the ^{13}C and ^{17}O chemical shifts of the CO-labeled heme proteins and the ν_{CO} infrared vibrational frequency. As the ν_{CO} is linearly altered by the EF projection along the bond (vibrational Stark effect), the chemical shift/EF linear dependence was obvious. That work was followed by a series of papers, where ^{19}F-shieldings in the fluorine-substituted proteins were successfully described in terms of the long-range electrostatic fields.[15,16] In the recent paper,[17] the application of vibrational Stark shifts of the nitrile infrared absorption signals in the ligand molecules was suggested as a detector of EFs at the active sites of the enzymes. In all these cases some synthetic modifications have to be done, which let us incorporate only several detectors in one biomolecule. Therefore, the main source of the EF information in proteins is continuing to be the empirical calculations using the Poisson−Boltzmann formalism. Nowadays, it is being quite routinely used,[18−20] but the necessity to find the way for their validation still exists. Another aspect of protein electric properties (their evolution and dynamic picture) is also still unclear, and this problem cannot be solved without certain experimental method for EF measurement in molecular level.

Thus, the study of the EF effects on the NMR parameters not only holds a theoretical importance but also is stimulating for a practical goal: search of the universal and convenient molecular spies for experimental EF measurement and visualization in biomolecules.

In this study we aim to partially fill the gap in the understanding of an EF influence on the indirect spin−spin couplings, providing computational results for a wider range of molecules, thus having an opportunity to make general conclusions. The one-bond *J*-couplings and particularly the $^1J_{NH}$ couplings in the model peptides are more concentrated on for the ideal EF detector search, as they are more convenient to find a connection with the molecular properties, rather than geometry. The peptide fragment was modeled by the *N*-methylformamide (NMF) and *N*-methylacetamide (NMA) molecules: an approach widely used before for theoretical penetration into the physicochemical insights of the amide group vibrational properties in peptides and proteins.[21−24]

2. Computational Details

The rapid development of computational methodologies made possible to study the indirect spin−spin coupling constants with almost experimental precision.[3,4,25,26] However, the necessity in triplet excitations requires the inclusion of more advanced theories, rather than the standard Hartree−Fock approach. Multiconfigurational self-consistent field methods as well as coupled-cluster methods[4,27,28] provide satisfactory results, but recently we were the witnesses of the increasing interest in the density functional theory (DFT) methods for computing indirect spin−spin coupling constants.[29−31] This tendency is determined by the lower computational cost of the method along with the indirect inclusion of the electron correlation effects. This makes DFT a valuable tool for *J*-coupling computations in large systems with a great promise for biomolecules.[32]

As a main tool in the current systematic study of the EF effect on the *J*-coupling constants, a hybrid-DFT[33] approach was chosen with the Becke's three-parameter hybrid functional and the Lee, Yang, and Parr correlation functional.[34−36] The performance of the B3LYP hybrid-DFT approach is considered to be the best for the spin−spin coupling evaluations in many molecules.[37,38] The basis sets were selected taking into account our previous study,[39] where a number of basis sets had been tested against the quality of the representation of the seven distinct coupling constants ($^1J_{CH}$, $^2J_{CH}$, $^3J_{NH}$, $^1J_{CC}$, $^1J_{CN}$, $^2J_{HH}$, $^2J_{CN}$) in acetonitrile. Applying that experience, the B3LYP/TZVP//B3LYP/6-31G(d,p) scheme was chosen, according to which *J*-coupling computations were performed using the TZVP basis of Ahlrichs and co-workers[40] on geometries optimized using the split-valence 6-31G(d,p) basis set.[41] All the calculations were done using the Gaussian 03 computational suite.[42]

The computations were composed of six parts with the subsection numbers in correspondence with numbers in the third section:

2.1. Study of External EF Effect on One-Bond *J*-Couplings in Several Molecules. External EF effect was studied on propane, acetonitrile and NMF (Figure 1) to understand the influence of the direction and the sign of the applied EF on various types of *J*-couplings. The calculations of the corresponding *J*-couplings were performed in the presence of external uniform EF ranging from −0.02 to +0.02 au (from −102.844 to +102.844 MV/cm)[43] (Tables 1 and 2). The MV/cm unit will be used throughout the article to make the presented results easily comparable to the EF evaluations in biomolecules. EFs applied along the internuclear vector and the orthogonal directions were considered (Figure 1). The geometries were taken from the optimization without external EF and kept frozen in the mentioned range of applied EFs for the single-point *J*-coupling calculations.

2.2. Study of EF Effects on Ramsey's Terms of $^1J_{NH}$ Coupling. According to Ramsey's formulation, the indirect spin−spin coupling constant between the interacting nuclei can be split into five contributions arising from the perturbation theory.[44] A thorough discussion of the theoretical aspects of *J*-couplings is out of the scope of this work and can be found in the references mentioned above.

A comparative analysis has been carried out to reveal the influence of the external uniform EF on the four (FC, Fermi

TABLE 1: Calculated One-Bond Spin−Spin Coupling Constants in Propane and Acetonitrile vs Applied Electric Field[a]

F_{CC}^{ext}/MV cm^{-1} [a]	$^1J_{CC}$/Hz		$^1J_{CH}$/Hz
	propane	acetonitrile	acetonitrile
−102.84	33.11	70.48	125.71
−51.42	34.08	68.14	128.84
−25.71	34.34	66.63	130.42
−10.28	34.43	65.64	131.38
−5.14	34.45	65.29	131.70
0	34.46	65.11	131.99
5.14	34.47	64.36	132.33
10.28	34.47	64.23	132.66
25.71	34.43	63.12	133.63
51.42	34.24	61.18	135.26
102.84	33.34	57.28	138.49

[a] The field was applied along the C−C bond in the corresponding molecule.

TABLE 2: Electric Field Effects on $^1J_{NH}$ Coupling and Its Ramsey's Terms in the *N*-Methylformamide

electric field/MV cm^{-1} [a]			indirect spin-spin coupling/Hz				
F_{NH}^{ext}	F_{NH}^{ind}	F_{NH}^{int}	$^1J_{NH}^{total}$	$^1J_{NH}^{FC}$	$^1J_{NH}^{SD}$	$^1J_{NH}^{PSO}$	$^1J_{NH}^{DSO}$
−102.84	15.47	−11.04	−98.07	−95.81	−0.066	−1.825	−0.370
−51.42	7.71	−18.80	−94.55	−91.94	−0.090	−2.140	−0.382
−25.71	3.85	−22.65	−92.75	−89.94	−0.109	−2.312	−0.388
−15.43	2.31	−24.19	−92.03	−89.14	−0.118	−2.385	−0.390
−10.28	1.54	−24.96	−91.67	−88.73	−0.123	−2.421	−0.391
−5.14	0.77	−25.73	−91.30	−88.32	−0.128	−2.459	−0.392
0	0	−26.50	−90.94	−87.91	−0.133	−2.497	−0.394
5.14	−0.76	−27.26	−90.57	−87.50	−0.139	−2.535	−0.395
10.28	−1.53	−28.03	−90.21	−87.09	−0.145	−2.574	−0.396
15.43	−2.30	−28.80	−89.84	−86.68	−0.151	−2.614	−0.397
25.71	−3.83	−30.33	−89.11	−85.85	−0.164	−2.695	−0.400
51.42	−7.64	−34.14	−87.27	−83.76	−0.201	−2.909	−0.406
102.84	−15.16	−41.66	−83.65	−79.53	−0.303	−3.392	−0.419

[a] F_{NH}^{ext} external uniform electric field was applied along the N−H bond with the H atom pointed in positive direction. Corresponding F_{NH}^{ind} induced and F_{NH}^{int} internal fields are also presented.

contact; SD, spin-dipole; PSO, paramagnetic spin−orbit; and DSO, diamagnetic spin−orbit) terms of the *J*-coupling constant. The constituents of the $^1J_{NH}$ coupling were analyzed on NMF with the methodology presented in the section 2.1 (Table 2). The external EF was aligned along the N−H bond with the hydrogen atom pointing in the positive direction.

2.3. Study of the Relationship between the External and Internal EFs. The interconnection between the externally applied uniform EF and the internal fields acting at the N−H site of the NMF molecule is examined via the comparison of the applied uniform EF values with the one computed from the DFT density (Table 2). The calculations were done with the same methodology presented in the section 2.1, retrieving also the EF values from the computed density (by the Prop keyword in Gaussian program). The latter gives the sum of the internal EF determined by naturally occurring electronic polarization, external EF (if applied), and the induced EF owing to the induced extra polarization (if the external EF presents). EF projections acting on the nitrogen atom along the N−H bond with the hydrogen atom pointing in the positive direction were considered.

2.4. Study of Internal EF Effects on $^1J_{NH}$ Couplings in Different Molecules. A set composed of 10 N−H containing molecules was chosen to obtain various internal EF values at the N−H moiety without an artificial external EF application. This set (set A mentioned in the Table 3) includes ammonia, various aliphatic and aromatic amines and amides. The molecules were calculated as described above but without external uniform EF. Geometry optimization with B3LYP/6-31G(d,p) method and the followed single point B3LYP/TZVP computations were done with tight convergence criteria. A comparison of the calculated *J*-couplings with the experimental ones available from the literature[45,46] was done for the selected set of molecules.

TABLE 3: Calculated N−H Bond Lengths, F_{NH}^0 Internal Electric Fields in the Absence of the Applied External Field, Calculated and Experimental $^1J_{NH}$ Coupling Constants for the Molecules Included in Set A

set A	r_{NH}/Å	F_{NH}^0/MV cm^{-1}	$^1J_{NH}^{calc}$/Hz	$^1J_{NH}^{exp}$/Hz[a]
NH_3	1.0180	−89.93	−54.32	−61.2
CH_3NH_2	1.0172	−81.94	−58.21	−64.5
$(CH_3)_2NH$	1.0165	−72.45	−62.82	−67
CH_3NHNO_2	1.0086	−26.39	−87.07	−100
$HCONH_2$-*syn*	1.0094	−6.10	−88.45	−88.3
anti	1.0072	−22.07	−90.39	−92.7
$HCONHCH_3$-*anti*	1.0084	−26.50	−90.94	−92.6
CH_3CONH_2-*syn*	1.0086	−6.01	−88.76	−88.4
anti	1.0061	−23.38	−89.77	−90.9
$PhNH_2$	1.0110	−45.04	−74.70	−78
o-$BrPhNH_2$	1.0095	−37.00	−78.90	−81.4
H near Br	1.0109	−26.02	−80.31	−81.4
$PhCONH_2$-*syn*	1.0099	−18.85	−84.75	−89
anti	1.0080	−32.41	−83.46	−89

[a] See refs 45 and 46.

TABLE 4: Calculated N−H Bond Lengths, $^1J_{NH}$ Couplings, F_{NH}^0 Internal Electric Fields and Hydrogen-Bonding Information for Various X-Substituted[a] *N*-Methylacetamides (NMA) Included in Set B (Figure 2)

no.	set B	r_{NH}/Å	F_{NH}^0/MV cm^{-1}	$^1J_{NH}^{calc}$/Hz	H-bond[b]
1	−H	1.0070	−26.49	−90.68	
2	−F	1.0094	−15.69	−91.69	
3	−Cl	1.0097	−13.95	−91.81	
4	−Br	1.0104	−12.48	−91.83	
5	$-CH_3$	1.0082	−26.87	−89.09	
6	$-NH_2$	1.0086	−25.38	−89.22	
7	−Ph	1.0083	−26.38	−89.08	
8	−*p*-ClPh	1.0081	−26.02	−89.39	
9	−*p*-BrPh	1.0081	−26.01	−89.39	
10	−*p*-FPh	1.0081	−26.18	−89.30	
11	−CHO	1.0083	−24.08	−90.03	
12	−CHO	1.0140	0.20	−92.19	1.96Å, 14.3^0
13	−CClO	1.0111	−5.47	−92.20	2.01Å, 14.8^0
14	$-NO_2$	1.0123	−4.48	−92.30	2.04Å, 15.6^0
15	$H_2O\cdots$NMA	1.0149	−3.20	−92.19	2.01Å, 1.1^0
16	$H_2O\cdots$NMA	1.0147	−2.82	−93.33	2.01Å, 1.7^0
17	a in *di*-NMA	1.0133	2.77	−94.60	1.98Å, 3.0^0
17	b in *di*-NMA	1.0074	−24.78	−91.25	

[a] $X-CH_2-CO-NH-CH_3$. [b] Hydrogen bond presence along with the H···O distance and NHO angle in the N−H···O moiety.

2.5. Study of Internal EF Effects on $^1J_{NH}$ Couplings in Substituted *N*-Methylacetamides. Similar as in section 2.4, calculations were done on various *N*-methylacetamides (NMA) (Table 4), where the acetylic methyl group was substituted by different substituents (set B). The chosen molecular set B (Figure 2) includes hydrogen bound H_2O-NMA complexes and the NMA-dimer (*di*-NMA) in a parallel orientation. Thus, the hydrogen bonding influence on the EF dependence of $^1J_{NH}$ coupling was also examined.

2.6. Study of the N−H Internuclear Distance and $^1J_{NH}$ Interconnection. The possible role of the N−H internuclear distance (Tables 3 and 4) was examined for all the studied molecules in both sets A and B. According to the selected scheme, the r_{NH} internuclear distances were taken from the B3LYP/6-31G(d,p) geometry optimizations with tight convergence criteria.

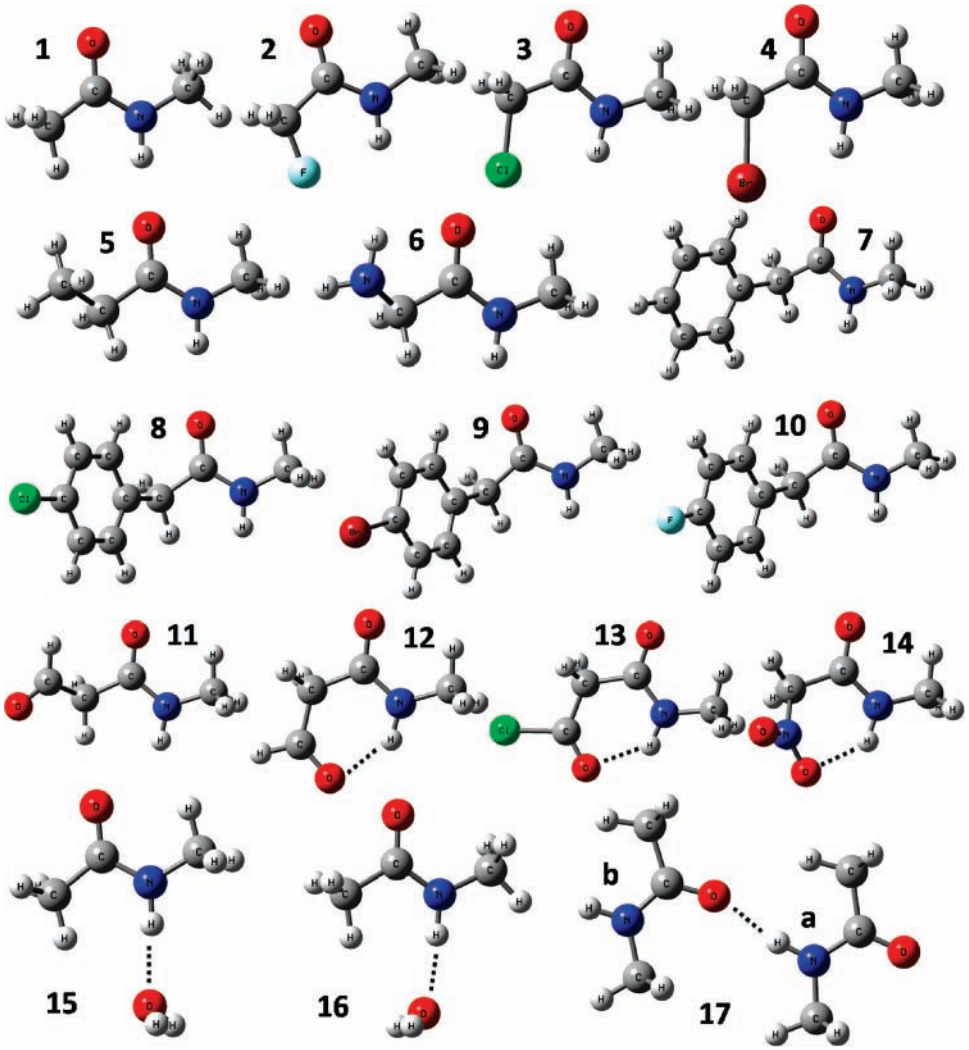

Figure 2. Optimized geometries of the molecules in set B. The numbering corresponds to the numeration in Table 4. Hydrogen bonds are shown by dots.

2.7. Study of the Angular Dependence of One-Bond *J*-Couplings and Internal Electric Fields. The methylamine, ammonia and formamide molecules were chosen to study the angular dependences of the one-bond *J*-couplings and internal EFs owing to the hyperconjugative interactions. In all the following calculations a tight convergence criteria were applied.

Methylamine molecule was first optimized by B3LYP/6-31G-(d,p) method with equalized C−H and N−H bond distances and HCN angles. Then the single point indirect spin−spin coupling and internal field calculations were done by the B3LYP/TZVP approach on the obtained structures while gradually rotating along the C−N bond.

The pyramidality effect was investigated on ammonia optimized by B3LYP/6-31G(d,p) method within the C_{3v} symmetry. Then the geometry was gradually changed altering only the angle between the symmetry axis and the N−H bonds without the change in symmetry. The B3LYP/TZVP single-point calculations were done on the obtained structures to get the $^1J_{NH}$ coupling and internal field values.

In the formamide molecule, the H−C−N−H torsion angle was frozen assigning gradually changing values starting from the *syn* arrangement of the N−H bond. The rest of the structure was optimized via the B3LYP/6-31G(d,p) method for each of the torsion angles changing the pyramidality of the nitrogen atom and followed by the single point $^1J_{NH}$ and internal field calculations via the B3LYP/TZVP method.

3. Results and Discussion

EFs affect the NMR parameters of the investigated molecule (i) via the interaction with the entire molecule as a whole unit and (ii) via the interaction in molecular level, leading to changes of some molecular properties such as electron density, charge distributions, etc.

As an example of the first type of interaction, an EF induced molecular alignment of the solute molecule can be mentioned. This can be described as applied EF−molecular dipole interaction, and the resulting molecular alignment affects the NMR spectrum of the solute molecules by the inclusion of anisotropic parameters (dipolar couplings, anisotropy of *J*-couplings, chemical shift anisotropy).

The second type is the EF interaction with the molecular components. As the electric field causes the electron cloud surrounding the nucleus of the atom to alter its position with respect to the nucleus, it leads to the alteration of NMR parameters. These effects are less studied; moreover, the majority of research refers to EF influence on chemical shifts. Hence the thorough study of EF effects on the *J*-couplings is well-timed.

Regardless of vicinal *J*-couplings, which have wide application in biomolecular NMR,[47] most of the one-bond *J*-couplings do not show any significant correlation with backbone and side chain geometrical parameters (for instance, with φ and ψ angles

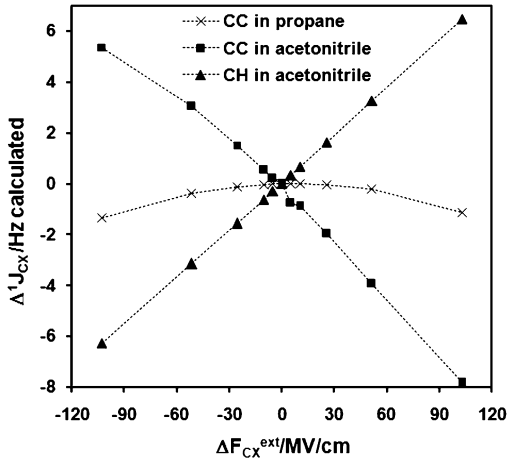

Figure 3. Change of the calculated *J*-couplings in propane and acetonitrile against the change of the applied electric field along the local symmetry axes.

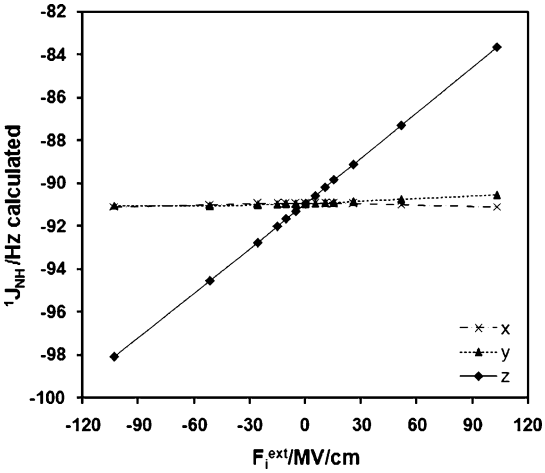

Figure 4. $^1J_{NH}$ coupling constant of *N*-methylformamide versus applied electric field in various directions as indicated in Figure 1.

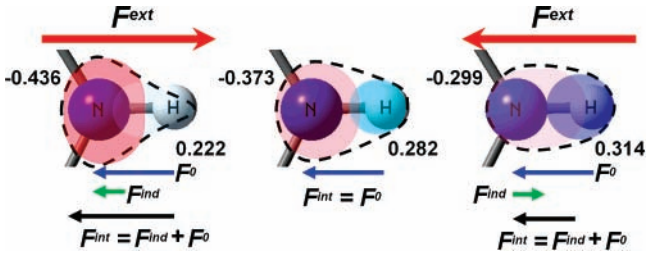

Figure 5. N−H site with all the types of electric field components along the bond. Numbers show the electrostatic potential fitted nuclear charges calculated for *N*-methylformamide without external electric field and with 102.8 MV/cm (0.02 au) external field applied in both parallel and antiparallel directions.

of protein backbone) and are not being used as restraints in protein structure refinements. The exceptions are $^1J_{C\alpha H\alpha}$[48,49] and $^1J_{C\alpha C\beta}$[50] couplings, for which several correlations with backbone geometry were found. Many types of the one-bond *J*-couplings can be potentially measured in biomolecules, and the study of their relation with the electrostatic properties at the corresponding sites is very promising idea which can lead to the full exploitation of the NMR measurable parameters with novel applications.

3.1. Electric Field Sign and Direction Sensitivity of the One-Bond *J*-Couplings. For a measurable parameter to be an EF detector, it should have a distinctive sign and direction sensitivity toward the EF. For several indirect spin−spin couplings, the sensitivity to the projection of the field along the local symmetry axis of the interacting nuclei was demonstrated.[11,12] That axis corresponds to the projection along the bond between the interacting nuclei for most of the cases. For the methylic $^1J_{CH}$ coupling, the main influence has the projection of the external field along the C−C bond as a local symmetry axis. In Figure 3, the changes of various one-bond *J*-couplings against the change in the external EF along the corresponding axes are plotted. A linear dependence is revealed for the $^1J_{CC}$ and $^1J_{CH}$ couplings in acetonitrile. However, the propane $^1J_{CC}$ coupling seems to be relatively inert against the change of the EF and only the absolute value of the EF is important for the observed weaker dependence. Thus, for a proper sign-sensitivity, the atoms of the interacting nuclei should be significantly different. It is particularly well demonstrated for the $^1J_{CC}$ couplings in acetonitrile and propane (Figure 3). In contrast to the acetonitrile, the two interacting carbons in propane molecule are not chemically different enough to possess a strong sensitivity toward the sign of the EF projection along the C−C bond. To this end, the heteronuclear one-bond *J*-couplings such as $^1J_{NH}$ and $^1J_{CH}$ are expected to be the most convenient EF detectors at their sites. Figure 4 presents the same external field vs *J*-coupling dependence for heteronuclear $^1J_{NH}$ constant in NMF, where the uniform field is externally applied along the N−H bond and orthogonal directions (Figure 1). The strong sensitivity toward the field along the bond can be noted again.

The NMF molecule was chosen to mimic the peptide bond in proteins. It should be noted that the biologically relevant EFs do not exceed tens of MV/cm[17,18] in contrast to the wider range applied in the calculations here. In the biologically relevant fields, the $^1J_{NH}$ coupling in the NMF is even less affected by the orthogonal to the bond components of the EF. Such a preferential sensitivity is very important for the possible implementation of one-bond *J*-couplings as an EF detector.

3.2. Electric Field Effects on Ramsey's Terms of $^1J_{NH}$ Couplings. Ramsey's formulation is a computationally convenient way to present indirect spin−spin coupling constants and in many cases the calculation of its constituent terms is the necessary part in research.

The results for NMF presented in Table 2 indicate about 16% change in $^1J_{NH}$ coupling within the studied EF range. That is prevalently determined by the FC term, which undergoes the 18.5% change under the same condition. The change of the rest SD, PSO and DSO terms, though have tiny contribution to the change of the total *J*-coupling, are very significant on their own with about 205, 63 and 13% distortions from their value in the absence of external EF.

3.3. Relation between the External and Internal Electric Field Effects on $^1J_{NH}$. In the absence of external EF, the electron density at the site of the interacting nuclei can be still polarized and this native polarization can be interpreted as an internal EF in the absence of external field (will be denoted as F^0). Hereafter, by saying EF, its projection along the bond between the nuclei of interest will be meant. External field leads to the electron density shift and extra polarization against the electric fieldlines, which causes an additional induced field (F^{ind}) to appear. The resulting internal EF (F^{int}) will be the sum of the induced and F^0 fields. This is schematically represented in Figure 5 for the $^1J_{NH}$ coupling in NMF. The numbers in the figure show the electrostatic potential fitted (Merz−Kollman) charges[51] for nitrogen and hydrogen atoms with and without 102.8 MV/cm external EF application in both directions. Screened by electrons, the nuclei will sense the internal field and the absolute dependence between the EF and one-bond

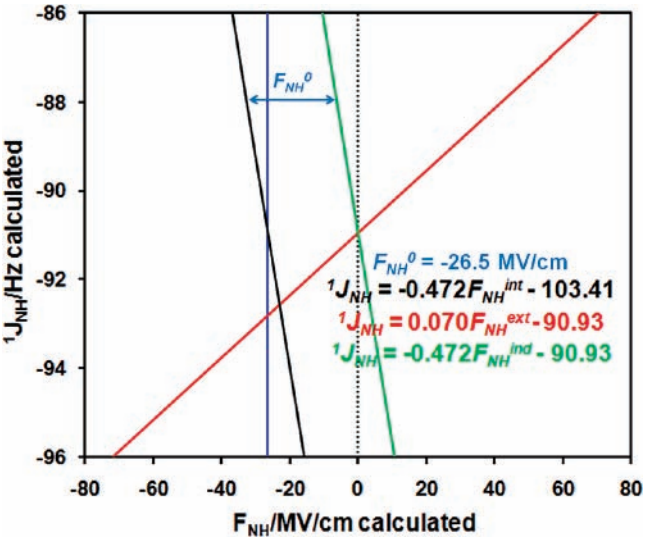

Figure 6. Interrelation between the $^1J_{NH}$ vs internal, external and induced electric field (along the N−H bond) dependences as computed for *N*-methylformamide. F_{NH}^0 value and the correlation equations are colored in correspondence with the trendlines: blue, internal field in the absence of external one; red, external field; green, induced field; black, internal field.

J-coupling should involve the internal F^{int} field rather than external one. The interconnection between the various (internal, externally applied and induced) EF effects on the $^1J_{NH}$ coupling is plotted in Figure 6. This graph was constructed using data from the calculations on NMF with the external EF application along the N−H bond and simultaneous determination of the EF values from the calculated density. The latter gives the sum of the external, induced and F^0 fields. For each of the trendlines ($R > 0.99$), 13 points were obtained. Within the frames of the theory and computational algorithm used in this study, the external field projection along the N−H bond induces 6.7 times weaker field in the opposite direction ($F_{NH}^{int} = F_{NH}^0 - 0.149F_{NH}^{ext}$).

The most surprising fact revealed is the same value (with only 0.2% deviation) of all the slope factors mentioned in the correlation equations in Figure 6 for a variety of molecules (ammonia, various substituted aliphatic and aromatic amines and amides). Thus, the EF dependence of the one-bond *J*-coupling seems to be a general property and for the $^1J_{NH}$ couplings the following generalized equation can be written:

$$^1J_{NH} = J - k(F_{NH}^0 + pF_{NH}^{ext}) \quad (2)$$

In this equation *J* is the characteristic N−H indirect spin−spin coupling constant, when the internuclear internal EF is equal to zero. That condition can be achieved by an external EF, which induces an equal to F_{NH}^0 field, but in the opposite direction. In our computational results *J* is close to −103 Hz. The coefficient *k* is equal to 0.472 Hz·cm/MV and describes the response of the corresponding *J*-coupling to the internal EF. The coefficient *p* describes the electronic polarizability along the bond and in current calculations is equal to −0.149. The pF_{NH}^{ext} term is the induced EF (F_{NH}^{ind}) projection along the bond, which has a negative sign. The $F_{NH}^0 + pF_{NH}^{ext}$ term is the F_{NH}^{int} internal EF and has always negative sign as in the naturally relevant conditions it is impossible to make the electrons of the N−H moiety spend more time near the hydrogen atom. Therefore, the resulting $^1J_{NH}$ coupling in any molecule is smaller in its absolute values than *J*. It should be noted that, in eq 2, the $^1J_{NH}$ coupling must be provided with a negative sign. The signs of the EF projections correspond to the case, when the hydrogen atom points to the positive direction. The numerical values of *k* and *p* coefficients are indicated for the calculated $^1J_{NH}$ and are relevant for only this particular method of calculation.

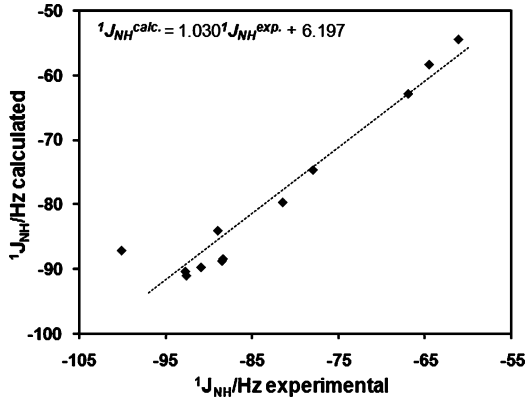

Figure 7. Correlation ($R = 0.962$) between the calculated and experimental $^1J_{NH}$ couplings for the molecules in set A.

These observations allow interpreting the sign-sensitivity of the one-bond *J*-couplings toward the external EF. *J*-coupling depends only on the internal field ($F_{ij}^{int} = F_{ij}^0 + pF_{ij}^{ext}$) which sign remains constant in naturally relevant region of the applied EF for N−H pair. However, when the electron densities at the interacting *i* and *j* atoms are closer to each other, the F_{ij}^0 field is very weak and the external EF can easily cause the change of the internal field sign. This is the case of $^1J_{CC}$ coupling in propane (Figure 3), where it was sensitive only to the absolute value of the external field. Thus, the correct sign of the external field projection can be represented only in cases, when the F_{ij}^0 field is strong enough for the internal field not being inversed by any naturally relevant induced fields. The latter condition is the key requirement for the *J*-coupling as an EF detector in macromolecules and fortunately is satisfied for the peptide $^1J_{NH}$ couplings.

3.4. Internal Electric Fields and the $^1J_{NH}$ Couplings of the Molecules in Set A. In the molecular set A (Table 3), simple molecules with reported experimental $^1J_{NH}$ values[45,46] were selected. There is a very good agreement between the calculated and experimental couplings (Figure 7). Set A includes molecules (for instance $PhCONH_2$), for which two different $^1J_{NH}$ couplings were calculated whereas experimentally they are observed as one. In these cases, the average computed coupling was taken for the comparison in Figure 7. Another imperfection of this comparison is the experimental dataset measured in various solvents with different dielectric constants which can substantially affect the couplings.[39] Taking into account the connection between the experimental and calculated couplings, a correction factor can be included in eq 2, and the empirical expression which links the B3LYP/TZVP//B3LYP/6-31G(d,p) computed EFs in MV/cm and the experimental $^1J_{NH}$ couplings can be written as:

$$^1J_{NH}^{exp} = -106.45 - 0.46(F_{NH}^0 - 0.149F_{NH}^{ext}) \quad (3)$$

The correlation between $^1J_{NH}$ coupling and the F_{NH}^0 field as computed for the molecules in set A without external EF application is plotted in Figure 8. The slope factor is very close to that computed for the separate molecules (eq 2, compare −0.449 and −0.472), which expresses the universality of the one-bond *J*-coupling vs EF dependence once again, pointing that EF along the interacting nuclei plays an important role in $^1J_{NH}$ coupling value formation.

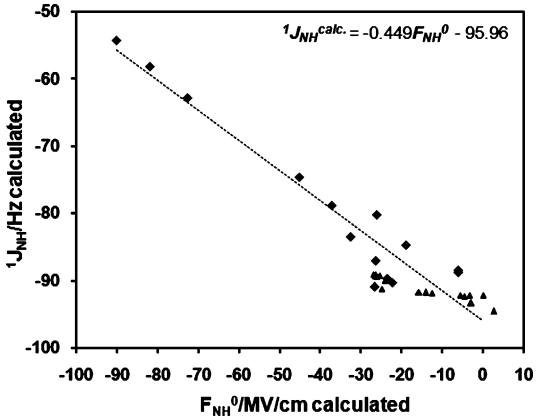

Figure 8. Correlation ($R = 0.957$) between the calculated $^1J_{NH}$ coupling constant and the nitrogen electric field projection along the N−H bond. The rhombs correspond to the molecules in set A and the triangles correspond to the substituted peptide moieties (set B).

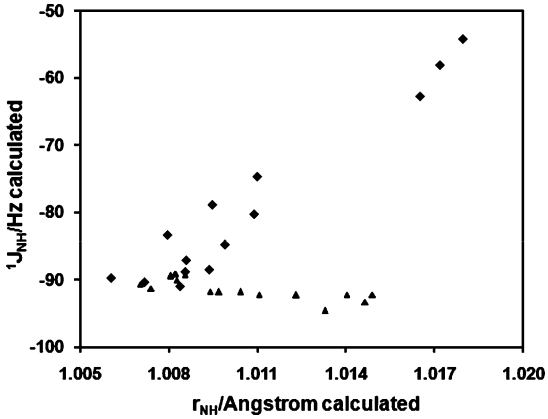

Figure 9. Calculated $^1J_{NH}$ coupling constant against the internuclear distance in angstroms for the optimized geometries. The rhombs correspond to the molecules in set A and the triangles to the substituted peptide moieties (set B).

3.5. Internal Electric Fields and the $^1J_{NH}$ Couplings of the Molecules in Set B and the Hydrogen Bonding Influence. The same computations were carried out for various peptide models included in set B (Figure 2, Table 4). Here, the core molecule was NMA and various substituents were attached to change the electrostatic state of the peptide fragment internally. Several hydrogen-bonded complexes (Figure 2) were also selected to check, whether the H-bonding causes deviations from the previously noted tendency. The results are presented in Figure 8 (triangles) jointly with the data from set A. From the general picture, a fairly good fit of the data to the outlined trend can be inferred. However, the sites of the molecular changes in set B are further from the amide moiety, than in set A, and the electrostatic field of the substituent partly acts as an external field. As the EFs computed without external EF application are not free from the small share of external and induced fields caused by the molecule itself, we can see a relatively weaker slope for the data for set B.

Hydrogen bonding does not express other influences and no any serious distortions are found. Though a small change in hydrogen bond geometry causes strong shift in the $^1J_{NH}$ coupling and F_{NH}^0, they keep being in accordance with the outlined dependence.

It was known that the frequency of the amine I mode in polypeptides and proteins are sensitive to the secondary structure.[52] Recently, high sensitivity of the same absorption band to the EF along the N−H bond was considered as an origin of the abovementioned phenomenon.[21−24] A very strong correlation was shown between the $^1J_{NH}$ coupling and IR stretching frequency of the amino group in para- and meta-substituted anilines.[53] Taking into account the vibrational Stark effect, all these facts are an indirect evidence for the strong and universal dependence between the one-bond *J*-couplings and the EF projection along the bond.

3.6. $^1J_{NH}$ Coupling and the N−H Internuclear Distance. The determination of the role played by N−H internuclear distance in the internal EF and $^1J_{NH}$ coupling formation is of principal importance to determine the primary factor affecting the *J*-coupling. Figure 9 presents the $^1J_{NH}$ coupling constant behavior against the internuclear distance for the molecules in sets A and B. All the calculations were performed with the same level of theory and precision. One can see a different behavior of data corresponding to the molecules in sets A and B. There is a correlation between *J*-coupling and N−H distance for the molecules of set A; however, the same correlation in set B is not very expressed and the slope has a different sign. Set A contains molecules with large variations of the internal EF value, and set B contains molecules with a smaller internal EF range, a similar neighborhood, but a large variation of distant groups. The $^1J_{NH}$ coupling increases with increasing internal EF for molecules of both sets, whereas the N−H distance increases for set A and decreases for set B with the increasing internal EF. The absence of any unified dependence between $^1J_{NH}$ and r_{NH} (Figure 9) in contrast to the distinct and universal behavior of the $^1J_{NH}$ and EF dependence (Figure 8) indicates the domination of the EF, rather than the internuclear distance in the formation of the corresponding one-bond *J*-coupling constant value.

3.7. Internal Electric Fields and the Angular Dependence of One-Bond *J*-Couplings. It was well studied fact that the $^1J_{XY}$ couplings can be split into the so-called (i) bond contribution involving the bond between the X and Y interacting atoms, (ii) other bond contributions involving only one of the X and Y atoms, and (iii) and lone electron pair (LP) contributions if applicable.[54] ^1J-couplings are greatly influenced by hybridization effects, orientation of nonbonding electron pairs and electron delocalization or hyperconjugative interactions (see ref 55 and the references therein). To this end, the universal character found for the $^1J_{NH}$ vs F_{NH}^0 dependence joining the corresponding couplings in ammonia, aromatic and aliphatic amines and amides faced a dilemma that could be solved only after thorough study of the angular dependence of the F_{NH}^0 fields themselves.

In case of N−H couplings, the most significant influence has the LP contribution from the nitrogen atom.[55,56] It always reduces the absolute value of the $^1J_{NH}$ coupling with the strength proportional to the s-character of the LP. In contrast, when the LP is of pure p-character as in planar amide groups, the LP contribution equals to zero.[56] This observation is reflected in the nitrogen pyramidality effect on the $^1J_{NH}$ couplings and explains the large absolute values of $^1J_{NH}$ in planar amides and aromatic amines in contrast to the smaller absolute values in pyramidal amines and ammonia.[56]

Three molecules (methylamine, ammonia and formamide as a peptide model) were chosen to study the angular dependence of $^1J_{NH}$ couplings and F_{NH}^0 internal field caused by the abovementioned effects. The angular dependences of ^1J-couplings were studied for all these molecules before (see ref 55 and the references therein), but here we repeat those calculations using our selected computational scheme and adding the angular dependence data for F_{NH}^0 internal field projections. For the

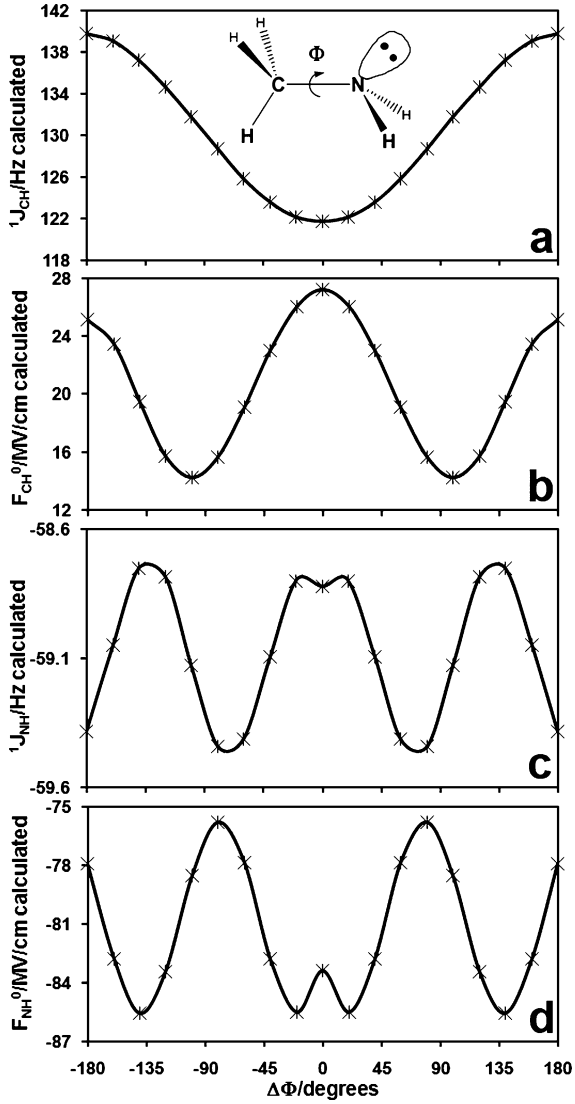

Figure 10. Angular dependence of the $^1J_{CH}$ and $^1J_{NH}$ couplings (a and c) in methylamine accompanied with the same angular dependences for the corresponding $F_{CH}{}^0$ and $F_{NH}{}^0$ internal field projections (b and d) along the C−H and N−H bonds and acting at carbon and nitrogen atoms respectively. The $\Delta\Phi = 0°$ dihedral angle corresponds to the antiperiplanar arrangement of the C−H bond and the nitrogen lone electron pair.

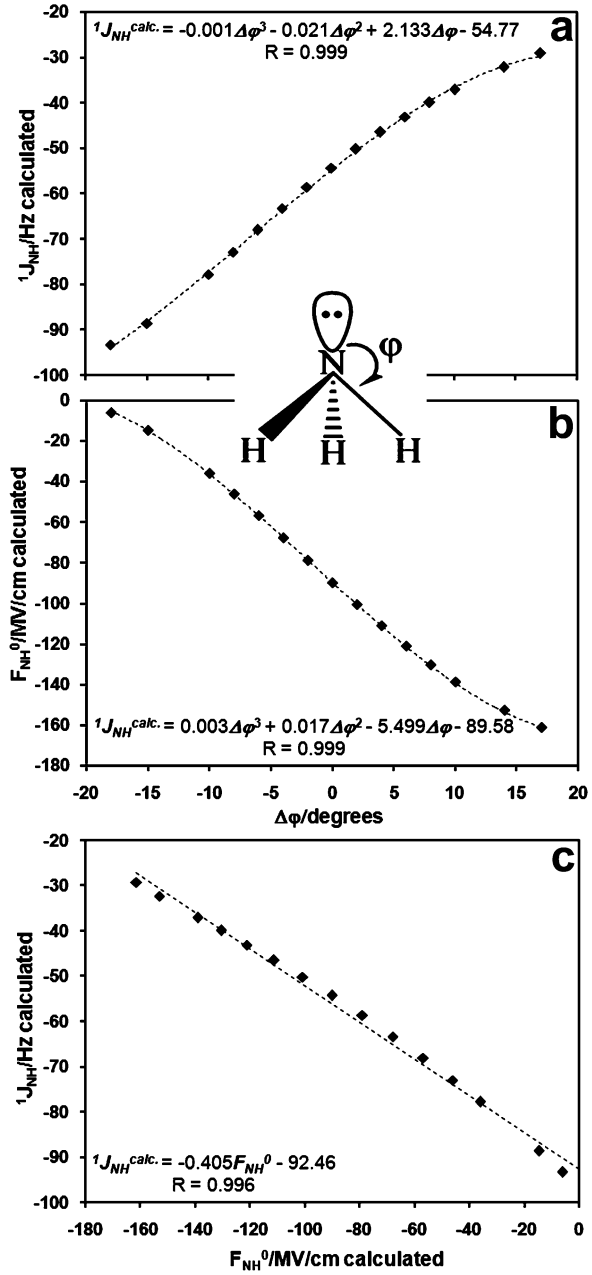

Figure 11. Nitrogen pyramidality effects on the $^1J_{NH}$ coupling (a) and the $F_{NH}{}^0$ internal field (b) values accompanied with the $^1J_{NH}$ vs $F_{NH}{}^0$ dependence graph (c) during the same pyramidality alteration. The $\Delta\varphi = 0°$ corresponds to the optimized structure of ammonia.

computational details, see the corresponding section and Supporting Information for the numerical results of the performed calculations.

In Figure 10a the angular dependence of $^1J_{CH}$ coupling in methylamine is plotted, where $\Delta\Phi = 0°$ torsion angle corresponds to the antiperiplanar arrangement of the C−H bond and nitrogen LP. The Perlin effect owing to the hyperconjugative interaction between the LP and C−H antibond[55] is demonstrated in this graph reaching its maximum influence in antiperiplanar ($\Delta\Phi = 0°$) conformation. If we consider the same angular dependence for the $F_{CH}{}^0$ internal EF projection along the C−H bond (Figure 10b), an interesting behavior different from the $^1J_{CH}$ angular dependence can be revealed. Because of this difference the $^1J_{CH}$ vs $F_{CH}{}^0$ dependence is not linear; thus the share of the hyperconjugative interactions should be taken into account when exploring the EF influence on the C−H couplings in nonflexible structures. However, examining the abovementioned dependence for $^1J_{NH}$ couplings and $F_{NH}{}^0$ fields, one can state the similar behavior (Figure 10c,d) of their angular dependences, which results in a linear ($R = 0.934$) $^1J_{NH}$ vs $F_{NH}{}^0$ dependence. On the other hand, the angular dependence of the $^1J_{NH}$ constants in methylamine is extremely weak.

The nitrogen pyramidality effect on the $^1J_{NH}$ coupling and $F_{NH}{}^0$ field in ammonia is reflected in Figure 11a,b, respectively. The pyramidality is presented via the $\Delta\varphi$ values (see the drawing in Figure 11), where the optimized ground state structure within the C_{3v} symmetry was taken ($\varphi_0 = 112.98°$ according to the selected computational scheme) as a reference. The pyramidality effect on the $^1J_{NH}$ couplings can be fully accounted by the $F_{NH}{}^0$ internal field, as the $^1J_{NH}$ vs $F_{NH}{}^0$ relation is almost linear (Figure 11c) with the slope factor very close to the one determined using the different molecules as the way to change internal EF at N−H sites (compare −0.405 with the −0.449 in Figure 8).

Taking into account the perspective to use the unique EF vs $^1J_{NH}$ dependence to measure EFs in biomolecules, the peptide

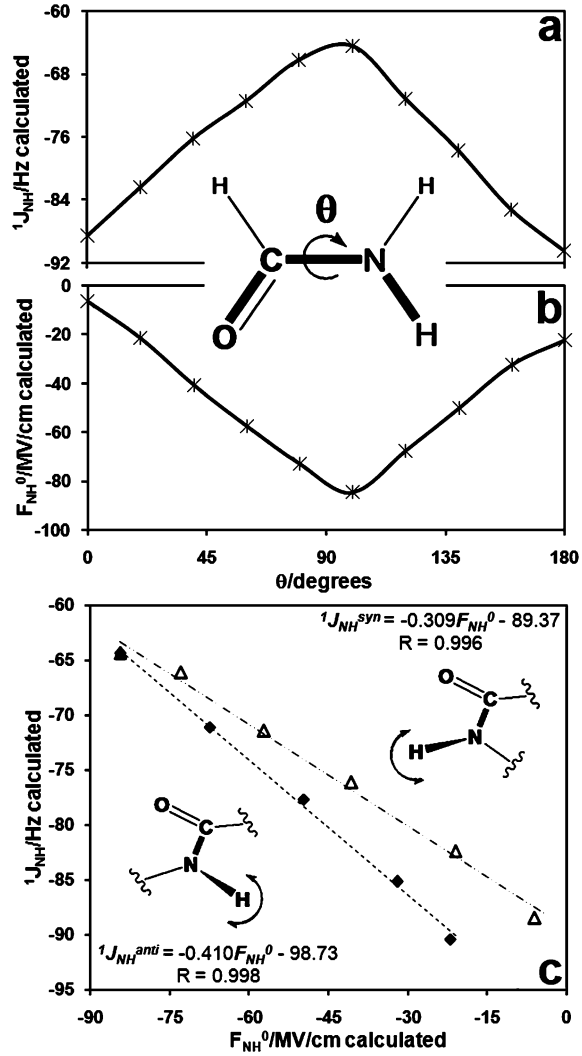

Figure 12. Change in the $^1J_{NH}$ couplings (a) and F_{NH}^0 internal field values (b) against the rotation along the C−N bond in formamide molecule with the rest of the structure optimized at each point. The graph presenting the linear $^1J_{NH}$ coupling vs F_{NH}^0 field dependence (c) during these structural changes is included. The $\theta = 0°$ angle corresponds to the *syn* arrangement of the N−H bond.

group was the focus of our attention. Because of the existence of carbonyl group in the peptide moiety, the conjugative interactions are taking place between the nitrogen LP and the carbonyl π-type bond (antibond). However, out-of-plane distortions of the N−H bond can weaken that conjugation, which will lead to the increase in the pyramidality of the nitrogen.

To examine that process under the light of the EF influence, the formamide molecule was taken as a peptide model and the angular dependence of the $^1J_{NH}$ and F_{NH}^0 was calculated. The formamide molecule was studied before to reveal the angular dependence of the $^1J_{NH}$ coupling constant,[55] but here the internal field calculations are also included. As θ, the angle for rotation, the O−C−N−H dihedral angle is selected and the $\theta = 0°$ corresponds to the *syn* arrangement of the N−H bond. $\theta = 180°$ corresponds to the *anti* form, which is the case of the peptide conformation in biomolecules. The results displayed in Figure 12 represent the similar behavior of the $^1J_{NH}/\theta$ and F_{NH}^0/θ dependences and again $^1J_{NH}$ coupling depends on the F_{NH}^0 internal field linearly with the previously outlined −0.410 slope factor for the *anti* conformation and not very different −0.309 slope factor for the *syn* form. The small difference in the slope factors of *anti* and *syn* forms is interesting on its own. In principle, a hyperconjugative interaction is possible between the N−H bond and the carbonyl group of the adjacent peptide group; however, the computations on dipeptide models with ϕ and ψ angle variations resulted in the outlined linear dependence again.[57]

Strengthening our assumption, all these results show that the hyperconjugative interactions, pyramidality and other phenomena are reflected in the internal F_{NH}^0 field variations and the $^1J_{NH}$ coupling constants can be fully accounted by the EF values at their sites.

3.8. EF Effects on *J*-Couplings and Possible Influence on EF NMR. Applied EF interaction with the molecules induces a partial molecular alignment along the field. The external EF induced alignment has been deeply studied since the early 60s of the last century by the Buckingham's[7−9] and MacLean's groups (see refs 58 and 59 and the references therein). They demonstrated the usefulness of the EF NMR for studying the insights of the isotropic and anisotropic molecular properties in liquid phase. However, for extracting the dipolar couplings of the aligned molecules, one should subtract isotropic *J*-couplings from the observed splittings in the spectra obtained by EF NMR. As the isotropic *J*-couplings are also sensitive to EFs, it is of particular importance to clarify how much the EF vs *J*-coupling dependence will influence the extracted dipolar couplings, which are being used to retrieve structural information of the molecules.

The usual strength of the applied electric field in EF NMR does not exceed 0.1 MV/cm with the general value of about 50 kV/cm. Thus, direct EF effect on the spin−spin couplings can be neglected under the influence of similar fields, as from our computations we expect just 0.007 Hz alteration of the $^1J_{NH}$ coupling constant when the N−H bond is aligned along the 0.1 MV/cm external field. However, weak electric fields can affect *J*-couplings via small geometry and vibrational distortions, which awaits detailed theoretical evaluations.

4. Conclusion

In the current work, the EF effect on the one-bond indirect spin−spin coupling constant is investigated. The study accentuates the $^1J_{NH}$ couplings with the background aim to implement the possibility to map the EFs in biomolecules by NMR spectroscopy. The role of the EF sign and direction, internal and induced components, hydrogen bonding and internuclear distance in the *J*-coupling formation were analyzed and the following general conclusions made.

1. If the bound atoms possess sufficiently different electron densities and an EF determined by the native electronic polarization (F_{ij}^0) exists along the bond, the corresponding one-bond *J*-coupling will be sensitive to the external EF projection with a linear dependence.

2. The most affected by the EF component of the $^1J_{NH}$ coupling constant is the spin-dipole term, although in the total *J*-coupling formation, the EF influence on the Fermi contact term is the most significant.

3. The absolute EF dependence of the one-bond *J*-coupling involves only the internal field, which is the sum of the induced field (if the external field exists) and the internuclear field determined by the native polarization. This dependence seems to be a general property of the interacting nuclei for a wide variety of molecules (see eq 3).

4. The correct sign of the external field projection can be represented only in cases, when the F_{ij}^0 field is strong enough for the internal field not being inversed by any naturally relevant induced fields.

5. If the N−H moiety of the molecule is involved in hydrogen bond, a small change in hydrogen bond geometry (i.e., distance and angular parameters) causes strong shift of the $^1J_{NH}$ coupling and F_{NH}^{int} field; however, the changes keep being in accordance with the outlined linear dependence.

6. The change in the internuclear distance affects the $^1J_{NH}$ coupling and the EF projection along the bond. However, the internal EF is the primary factor defining the values of the *J*-couplings, as there are many molecules, among which the computed internuclear distances are widely changing while the corresponding couplings as well as the internal EFs are more conservative.

7. The hyperconjugative interactions, pyramidality and other angular dependence phenomena are reflected in the internal F_{NH}^0 field variations and the $^1J_{NH}$ coupling constants can be fully accounted by the EF value at their sites.

8. The peptide $^1J_{NH}$ coupling constants have a potential to serve as an EF detector in biomolecules after their thorough experimental calibration. The latter can be performed using the vibrational Stark effect on the amide absorption frequencies of any model peptide by the IR spectroscopy, where the external EF can be applied more conveniently, than in conventional NMR spectrometers. Followed by the study of the interconnection between the $^1J_{NH}$ couplings and amide IR bands, the experimental calibration of the $^1J_{NH}$ couplings against the external EFs can be performed.

9. The direct EF effects on the spin−spin couplings in the EF NMR are negligible due to the weaker strength of the field; however, it can affect *J*-couplings via small geometry and vibrational distortions, which awaits detailed theoretical evaluations.

It is very challenging to search an experimental method for EF measurement, but finding it among NMR parameters will be more exciting, because the EF information can be more conveniently extracted from standard NMR experiments during protein geometry determination. Furthermore, NMR provides an opportunity to study protein dynamics and folding; thus such a detector can lead to simultaneous determination of electrostatic potential evolution during those processes.

Acknowledgment. This work was supported by U.S. Civilian Research and Development Foundation through the ARB2-2834-YE-06 award. A. B. Sahakyan is grateful to the National Foundation of Science and Advanced Technologies (NFSAT) for their TGP2006/05 travel grant.

Supporting Information Available: Tables presenting the numerical results of the calculations reflected in Figures 10−12 ($^1J_{CH}$ and $^1J_{NH}$ couplings and F_{CH}^0 and F_{NH}^0 internal fields). This information is available free of charge via the Internet at http://pubs.acs.org.

References and Notes

(1) Oldfield, E. *J. Biomol. NMR* **1995**, *5*, 217.
(2) Case, D. A. *Curr. Opin. Struct. Biol.* **2000**, *10*, 197.
(3) Contreras, R. H.; Peralta, J. E.; Giribet, C. G.; de Azúa, R.; Facelli, J. C. *Annu. Rep. NMR Spectrosc.* **2000**, *41*, 55.
(4) Vaara, J.; Jokisaari, J.; Wasylishen, R. E.; Bryce, D. L. *Prog. NMR Spectrosc.* **2002**, *41*, 233.
(5) Stephen, M. *J. Mol. Phys.* **1957**, *1*, 223.
(6) Grayson, M. In *Recent Research Developments in Physical Chemistry*; Transworld Research Network: Trivandrum, India, 2002; Chapter 6, pp 469−494.
(7) Buckingham, A. D. *Can. J. Chem.* **1960**, *38*, 300.
(8) Buckingham, A. D.; Lovering, E. G. *Trans. Faraday Soc.* **1962**, *58*, 2077.
(9) Buckingham, A. D.; Pople, J. A. *Trans. Faraday Soc.* **1963**, *59*, 2421.
(10) Barfield, M.; Johnston, M. D. *Chem. Rev.* **1973**, *73*, 53.
(11) de Kowalewski, D. G.; Kowalewski, V. J.; Peralta, J. E.; Eskuche, G.; Contreras, R. H.; Esteban, A. L.; Galache, M. P.; Diez, E. *Magn. Reson. Chem.* **1999**, *37*, 227.
(12) Grayson, M. *Int. J. Mol. Sci.* **2003**, *4*, 218.
(13) Villa, J.; Warshel, A. *J. Phys. Chem. B* **2001**, *105*, 7887.
(14) Augspurger, J. D.; Dykstra, C. E.; Oldfield, E. *J. Am. Chem. Soc.* **1991**, *113*, 2447.
(15) Pearson, J. G.; Oldfield, E.; Lee, F. S.; Warshel, A. *J. Am. Chem. Soc.* **1993**, *115*, 6851.
(16) de Dios, A. C.; Pearson, J. G.; Oldfield, E. *Science* **1993**, *260*, 1491.
(17) Suydam, I. T.; Snow, C. D.; Pande, V. S.; Boxer, S. G. *Science* **2006**, *313*, 200.
(18) Honig, B.; Nicholls, A. *Science* **1995**, *268*, 1144.
(19) Warshel, A.; Papazyan, A. *Curr. Opin. Struct. Biol.* **1998**, *8*, 211.
(20) Simonson, T. *Curr. Opin. Struct. Biol.* **2001**, *11*, 243.
(21) Torii, H.; Tasumi, M. *Int. J. Quantum Chem.* **1998**, *70*, 241.
(22) Torii, H.; Tatsumi, T.; Kanazawa, T.; Tasumi, M. *J. Phys. Chem. B* **1998**, *102*, 309.
(23) Ham, S.; Kim, J.-H.; Lee, H.; Cho, M. *J. Chem. Phys.* **2003**, *118*, 3491.
(24) Torii, H. *J. Phys. Chem. A* **2004**, *108*, 7272.
(25) Vahtras, O.; Ågren, H.; Jørgensen, P.; Jensen, H. J. A.; Padkjær, S. B.; Helgaker, T. *J. Chem. Phys.* **1992**, *96*, 6120.
(26) Helgaker, T.; Jaszuński, M.; Ruud, K. *Chem. Rev.* **1999**, *99*, 293.
(27) Perera, S. A.; Sekino, H.; Bartlett, R. J. *J. Chem. Phys.* **1994**, *101*, 2186.
(28) Auer, A. A.; Gauss, J. *J. Chem. Phys.* **2001**, *115*, 1619.
(29) Malkin, V. G.; Malkina, O. L.; Salahub, D. R. *Chem. Phys. Lett.* **1994**, *221*, 91.
(30) Malkina, O. L.; Salahub, D. R.; Malkin, V. G. *J. Chem. Phys.* **1996**, *105*, 8793.
(31) Barone, V. In *Recent Advances in Density Functional Methods*; Chong, D. P., Ed.; World Scientific: Singapore, 1995; Vol. 1.
(32) Watson, M. A.; Salek, P.; Macak, P.; Jaszuński, M.; Helgaker, T. *Chem. Eur. J.* **2004**, *10*, 4627.
(33) Kohn, W.; Sham, L. J. *Phys. Rev. A* **1965**, *140*, 1133.
(34) Becke, A. D. *J. Chem. Phys.* **1993**, *98*, 5648.
(35) Lee, C.; Yang, W.; Parr, R. G. *Phys. Rev. B* **1988**, *37*, 785.
(36) Miehlich, B.; Savin, A.; Stoll, H.; Preuss, H. *Chem. Phys. Lett.* **1989**, *157*, 200.
(37) Helgaker, T.; Watson, M.; Handy, N. C. *J. Chem. Phys.* **2000**, *113*, 9402.
(38) Lantto, P.; Vaara, J.; Helgaker, T. *J. Chem. Phys.* **2002**, *117*, 5998.
(39) Sahakyan, A. B.; Shahkhatuni, A. A.; Shahkhatuni, A. G.; Panosyan, H. A. *Magn. Reson. Chem.* **2008**, *46*, 63.
(40) Schaefer, A.; Huber, C.; Ahlrichs, R. *J. Chem. Phys.* **1994**, *100*, 5829.
(41) Rassolov, V. A.; Ratner, M. A.; Pople, J. A.; Redfern, P. C.; Curtiss, L. A. *J. Comput. Chem.* **2001**, *22*, 976.
(42) Frisch, M. J.; Trucks, G. W.; Schlegel, H. B.; Scuseria, G. E.; Robb, M. A.; Cheeseman, J. R.; Montgomery, J. A.; Vreven, J. T.; Kudin, K. N.; Burant, J. C.; Millam, J. M.; Iyengar, S. S.; Tomasi, J.; Barone, V.; Mennucci, B.; Cossi, M.; Scalmani, G.; Rega, N.; Petersson, G. A.; Nakatsuji, H.; Hada, M.; Ehara, M.; Toyota, K.; Fukuda, R.; Hasegawa, J.; Ishida, M.; Nakajima, T.; Honda, Y.; Kitao, O.; Nakai, H.; Klene, M.; Li, X.; Knox, J. E.; Hratchian, H. P.; Cross, J. B.; Adamo, C.; Jaramillo, J.; Gomperts, R.; Stratmann, R. E.; Yazyev, O.; Austin, A. J.; Cammi, R.; Pomelli, C.; Ochterski, J. W.; Ayala, P. Y.; Morokuma, K.; Voth, G. A.; Salvador, P.; Dannenberg, J. J.; Zakrzewski, V. G.; Dapprich, S.; Daniels, A. D.; Strain, M. C.; Farkas, O.; Malick, D. K.; Rabuck, A. D.; Raghavachari, K.; Foresman, J. B.; Ortiz, J. V.; Cui, Q.; Baboul, A. G.; Clifford, S.; Cioslowski, J.; Stefanov, B. B.; Liu, G.; Liashenko, A.; Piskorz, P.; Komaromi, I.; Martin, R. L.; Fox, D. J.; Keith, T.; Al-Laham, M. A.; Peng, C. Y.; Nanayakkara, A.; Challacombe, M.; Gill, P. M. W.; Johnson, B.; Chen, W.; Wong, M. W.; Gonzalez, C.; Pople, J. A. *Gaussian 03*, revision B.01; Gaussian Inc.: Pittsburgh, PA, 2003.
(43) 1 au (atomic unit) of an electric field equals 5142.2064 MV/cm.
(44) Ramsey, N. F. *Phys. Rev.* **1953**, *91*, 303.
(45) Berger, S.; Braun, S.; Kalinowski, H.-O. *NMR Spectroscopy of the Non-Metallic Elements*; Wiley: Chichester, U.K., 1997; Chapter 4.
(46) Martin, G. J.; Martin, M. L.; Gouesnard, J.-P. *NMR Basic Princ. Prog.* **1981**, *18*, 1.
(47) Cavanagh, J.; Fairbrother, W. J.; Palmer, A. G.; Skelton, N. J. *Protein NMR Spectroscopy: Principles and Practice*; Academic Press: San Diego, 1996.
(48) Vuister, G. W.; Delaglio, F.; Bax, A. *J. Am. Chem. Soc.* **1992**, *114*, 9674.

(49) Mierke, D. F.; Grdadolnik, S. G.; Kessler, H. *J. Am. Chem. Soc.* **1992**, *114*, 8283.
(50) Cornilescu, G.; Bax, A.; Case, D. A. *J. Am. Chem. Soc.* **2000**, *122*, 2168.
(51) Besler, B. H.; Merz, Jr., K. M.; Kollman, P. A. *J. Comput. Chem.* **1990**, *11*, 431.
(52) Mantsch, H. H.; Casal, H. L.; Jones, R. N. In *Spectroscopy of Biological Systems*; Clark, R. J. H., Hester, R. E., Eds.; Advances in Spectroscopy, Vol. 13; Wiley: New York, 1986; p 1.
(53) Takasuka, M.; Terui, Y. *J. Chem. Soc., Perkin Trans.* **1984**, *2*, 1545.
(54) Contreras, R. H.; Ruiz De Azúa, M. C.; Giribet, C. G.; Aucar, G. A.; Lobayán,De Bonczok, R. *J. Mol. Struct. (THEOCHEM)* **1993**, *284*, 249.
(55) Contreras, R. H.; Peralta, J. E. *Prog. NMR Spectrosc.* **2000**, *37*, 321.
(56) Ruiz De Azúa, M. C.; Giribet, C. G.; Vizioli, C. V.; Contreras, R. H. *J. Mol. Struct. (THEOCHEM)* **1998**, *433*, 141.
(57) Sahakyan, A. B.; et al. Unpublished results.
(58) Hilbers, C. W.; MacLean, C. *NMR Basic Princ. Prog.* **1972**, *7*, 1.
(59) van Zijl, P. C. M.; Ruessink, B. H.; Bulthuis, J.; MacLean, C. *Acc. Chem. Res.* **1984**, *17*, 172.